Original article

# X-ray Diffraction, Electronic Circular Dichroism, and Quantum Mechanics (TD-DFT) Investigations on 4-Dehydroxyaltersolanol A, a Secondary Metabolite from Endophytic Fungus *Nigrospora oryzae*

Fatimah Bebe Mohamed Hussain[1,2] (iD), Sadia Sultan[1,3*] (iD), Imene Bayach[4], Humera Naz[1,3], Gurmeet Kaur Surindar Singh[1], Syed Adnan Ali Shah[1,3], Kamran Ashraf[1,3], Fatimah Salim[2,5], Jean-Frédéric Faizal Weber[1,2]

[1]Faculty of Pharmacy, Universiti Teknologi MARA Puncak Alam Campus, Bandar Puncak Alam, Kuala Selangor, Selangor, Malaysia.
[2]Atta-ur-Rahman Institute for Natural Product Discovery (AuRins), Universiti Teknologi MARA Puncak Alam Campus, Bandar Puncak Alam, Kuala Selangor, Selangor, Malaysia.
[3]Biotransformatiom Research Group (Health and Wellness), Faculty of Pharmacy, Universiti Teknologi MARA Puncak Alam Campus, Bandar Puncak Alam, Kuala Selangor, Selangor, Malaysia.
[4]Chemistry Department, College of Science, King Faisal University, Al-Hofuf, Saudi Arabia.
[5]Faculty of Applied Sciences, Universiti Teknologi MARA Shah Alam, Shah Alam, Selangor, Malaysia.

## Abstract

**Background and objectives**: A tetrahydro anthraquinone derivative, 4-dehydroxyaltersolanol A, has been obtained from *Nigrospora oryzae*, which was isolated from *Uncaria borneensis* Havil as an endophytic fungus. This is a recently described compound whose stereochemistry was assumed from biogenetic considerations. However, using ECD spectral analysis in combination with TD-DFT calculations, its stereochemistry could be determined unambiguously. **Method:** In the current research, the selected TH1P45 culture was analysed using semi-preparative HPLC, which led to the isolation of six secondary metabolites, including 4-dehydroxyaltersolanol A (**1**). We have further presented full evidence of the stereochemistry of compound **1**. With the help of quantum calculations, we also determined the mechanism by which this compound degrades in solution. **Results:** The analysis of TH1P45 culture led to the isolation of six secondary metabolites, including 4-dehydroxyaltersolanol A, three anthraquinone derivatives (macrosporin, bostrycin and altersolanol B), and two pyrones (pestalopyrone and hydroxypestalopyrone). **Conclusion:** A full evidence of the stereochemistry of compound 1 with the help of the combination of X-ray crystallography, ECD, and TD-DFT quantum calculations, allowed unambiguously assigning the absolute stereochemistry of 4 dehydroxyaltersolanol A as 1*S*,2*R*,3*S* as correctly assumed by Proksh and collaborators from biogenetic considerations.

**Keywords:** 4-dehydroxyaltersolanol A; DFT and TD-DFT studies; endophytes; *Nigrospora oryzae*

## Introduction

A novel tetrahydroanthraquinone derivative was isolated by Peter Proksch's group and named 4-

dehydroxyaltersolanol A [1]. It was obtained from the culture of *Nigrospora oryzae* isolated as

an endophyte from the African plant *Combretum dolichopetalum* Engl. & Diels. Endophytes are microorganisms that live in plants for at least a part of their life, usually without causing apparent symptoms. Among endophytic species, fungal endophytes constitute a rich source of bioactive secondary metabolites that are of interest for plant protection in addition to different medicinal and agrochemical applications [2]. As a result of an ongoing research in endophytes [3], examination of Malaysian *Uncaria borneensis* led to the isolation of, among others, another accession of *N. oryzae* coded TH1P45. *Nigrospora oryzae* is fast growing and best known as a mild pathogen for rice [4] as well as for sorghum, corn [5], and other crops [6-8]. It is also a saprotrophic fungus colonizing debris in living and dead plants [5], as well as endophytic to many plants [9-10]. Various isolates of this species were shown to produce a significant array of secondary metabolites, including phytotoxic, antimicrobial and plant biocontrol agents [11-13]. Over the course of research aimed at the discovery of bioactive natural products, the analysis of TH1P45 solid culture led to the isolation of six secondary metabolites including 4-dehydroxyaltersolanol A (**1**), pestalopyrone [14] (**2**), hydroxypestalopyrone [15] (**3**), macrosporin [16-19] (**4**), bostrycin [19-20] (**5**), and altersolanol B [19] (**6**) (Figures 1 and 2).

The elucidation of compound **1**'s plane structure was carried out by Uzor et al. [1] by conventional spectroscopic analysis, while its stereochemistry was only assumed by comparison with analogues present in the same extract using biogenetic considerations. Here, we present full evidence of the stereochemistry of compound **1**. With the help of quantum calculations, we also determined the mechanism by which this compound degrades in solution.

## Material and Methods
### Ethical considerations
This research has been approved and accepted by the research committee of Faculty Pharmacy UiTM and endorsed by Institute of post graduate UiTM during defense of research proposal (500-IPSis (8/6/9).

### Chemicals
Anhydrous sodium sulphate from Bendosen (Germany), 70 % ethanol and ethyl acetate AR from Fisher Scientific (UK), brine solution, and ultrapure water (18 MΩ.cm) generated by a water purification system from Elga (UK) were used in the study. The standard culture medium used for fungi was potato dextrose agar (PDA) from Merck (Germany). Deuterated NMR solvents acetone-d6 ($CD_3COCD_3$), chloroform-d ($CDCl_3$), (Almar Chemical, Switzerland) and methanol-d4 (MeOD) (Merck, Germany). Promega's Wizard® Genomic DNA Purification kit (cat. No. A1120) Promega's Wizard® SV Gel and PCR System (cat. No.: A9281, USA) were provided for the study.

### General experimental procedures
NMR spectra were recorded on a Bruker Ascend™ 600 spectrometer with Topspin™ 3.0 data acquisition software (Germany and Switzerland) in $CD_3OD$, $CDCl_3$, or acetone-d6. HR-ESI-TOF-MS analyses were performed with an Agilent 6224 TOF LC/MS instrument (Agilent Technologies, Germany). Optical rotations were measured on an A. Krüss Optronic P8000-T digital polarimeter. UV and ECD spectra were collected on a JASCO J-815-150S spectrometer, Japan. Semi-preparative HPLC was performed on an Agilent 1200 system using a C18 column Synergy Hydro-RP 80 Å 150 x 10 mm, 4 μm particles (Phenomenex®, USA). Analytical HPLC experiments were performed on an Agilent 1260 system equipped with a column of Synergy 4 μm Hydro-RP 80 Å 150 × 4.6 mm, 4 μm particles (Phenomenex®, USA).

### Isolation and identification of the fungal material
Fungal isolate *Nigrospora oryzae* TH1P45 was obtained from petals of *Uncaria borneensis* Havil. (Rubiaceae) collected in UiTM's Biological Reserve, Puncak Alam, Malaysia (GPS: 3.196553, 101.443024). An authenticated voucher specimen of the collected plant was deposited at the Herbarium of the Forest Research Institute of Malaysia (FRIM), Kepong, Malaysia (sample code: PID 490915-25). The petals were thoroughly washed, and surface sterilized by immersion in 70% ethanol for 1 min, 5% NaOCl for 3 min and 70 % ethanol for 30 s, followed by washing in sterile ultrapure water. The petals were then cut into small fragments over sterile filter paper and transferred to Petri plates onto potato dextrose agar (PDA)

supplemented with chlortetracycline hydrochloride (0.05 mg/100 mL) and streptomycin sulphate (0.25 mg/100 mL). The plates were incubated at 28 °C until fungal growth was observed. Growing mycelium was transferred on fresh PDA and stored on PDA slants at 4 °C until further study. Identification of the TH1P45 fungus was performed by observing mycelium and conidia by optical and scanning electron microscopy. It was confirmed by rDNA amplification and sequencing by means of Promega's Wizard® Genomic DNA Purification kit and Promega's Wizard® SV Gel and PCR Clean-Up System according to the manufacturer's protocols. The PCR product was then submitted for sequencing (1st Base Laboratories Sdn Bhd, Malaysia). The fungus was identified as *Nigrospora oryzae*, whose 446 base pair ITS sequence had 99% homology with
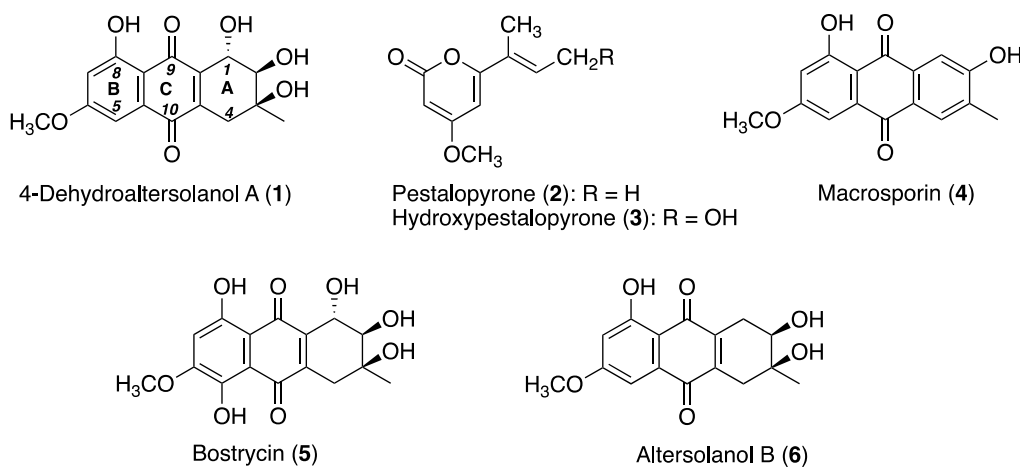
*N. oryzae* strain 62 (KP942835). This sequence was deposited at GenBank® as *N. oryzae* strain TH1P45 with accession number KX355828.

## Fermentation, extraction and compound isolation

Fungal isolate TH1P45 was inoculated on thirty 9-cm petri dishes containing 20 mL of PDA and incubated for 3 weeks at 28 °C. The fully grown cultures were homogenised with brine solution for 3-5 min at a rate of 7,000–9,000 rpm using an Ultra-Turrax® homogenizer (IKA, Germany). The homogenised mixture (1.5 L) was extracted three times with ethyl acetate (total 1.8 L) with the help of an overhead stirrer at 1100 rpm for 3 min. The organic layers were collected, dried over anhydrous sodium sulphate and evaporated under reduced pressure.
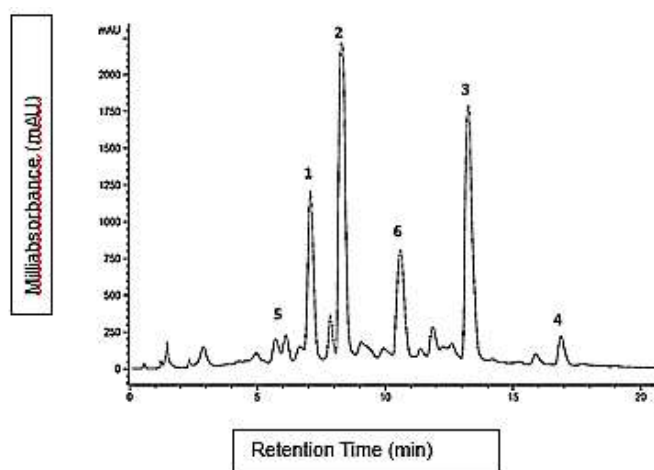


**Figure 1.** HPLC chromatogram of the extract of *Nigrospora oryzae* TH1P45 culture on potato dextrose agar; numerals refer to the isolated compounds.



4-Dehydroaltersolanol A (**1**)

Pestalopyrone (**2**): R = H
Hydroxypestalopyrone (**3**): R = OH

Macrosporin (**4**)

Bostrycin (**5**)

Altersolanol B (**6**)

**Figure 2.** Structures of the 4-dehydroxyaltersolanol A (**1**), pestalopyrone (**2**), hydroxypestalopyrone (**3**), macrosporin (**4**), bostrycin (**5**) and altersolanol B (**6**) isolated from *nigrospora oryzae* TH1P45.

The semi-preparative HPLC purification of compounds **1**-**6** was carried out as follows: 50 mg of the fungal extract was dissolved in 1 mL of methanol (MeOH). The sample was fractionated on a semi-preparative $C_{18}$ column at 5 mL/min by $ACN/H_2O$ gradient elution (ACN: 0 min: 10%; 10 min: 46 %; 15 min: 65%; 20 min: 100%; and 25 min: 100%). When necessary, further purification was achieved on an analytical column to obtain metabolites **1**-**6**.

### X-ray diffraction analysis of 1
Red-orange crystals of **1** were obtained from methanol and chloroform in a ratio 7:3 (v/v). The crystal data were collected on a Bruker APEX-2 CCD diffractometer using Mo Kα radiation. The structure was solved by direct methods using SHELXS-97 [21] and refined with full-matrix least squares calculations on F2. All nonhydrogen atoms were refined anisotropically. All hydrogen atoms were refined as riding on their parent atoms using SHELXL 2013 [22] defaults, except for those of the O1, O2, O3 and O6 (numbering as per Figure. 2) whose coordinates were refined from the starting coordinates obtained from a difference Fourier synthesis using a DFIX restraint for the O-H bond of 0.82 Å. Crystallographic data of **1** (excluding structure factors) has been deposited at the Cambridge Crystallographic Data Centre (CCDC) with the deposition number 1484016. A Copy of the data can be obtained free of charge from the CCDC, 12 Union Road, Cambridge CB2 1EZ, UK [fax: +44 (0) 1223-336033 or e-mail: deposit@ccdc.cam.ac.uk].

### Computational procedures
The conformational analysis showed four possible conformations for compound **1** that have a predicted Boltzmann population of ~ 2, 5, 20 and 70% in favour of conformer (2) followed by (3) for a more equal population depending on the functional and basis sets used. Geometry optimisation of the ground-state of all studied molecules has been carried out with the help of density functional theory (DFT) using the hybrid functional B3LYP, combined with the 6–311+G(d,p) basis set (B3LYP/6–311+G(d,p)). The frequency analyses were performed at 298 K and 1 atm at the same level of theory. No negative eigenvalue (i.e., no imaginary frequency) was obtained, confirming true ground states minima.

Time-dependant Density Functional Theory (TDDFT) calculations using the basis sets and functional stated for up to 250 states were used to simulate the electronic circular dichroism spectra. Comparison of ECD spectra for the conformational forms (2) and (3) that are very similar with other conformers indicated the only perceptible differences were a blue shift for conformers (2) and (3) in the 200–250 nm region and some small intensity differences.

DFT and TD-DFT calculations for 4-dehydroxyaltersolanol A (**1**) were performed in solvent, while the calculation of the protonated species (Figure 8) was completed in gas phase. The solvent effect was considered implicitly using a polarizable continuum model (PCM), in which the solute was embedded in a shape-adapted cavity surrounded by solvent described as a dielectric continuum characterised by its dielectric constant. The PCM in TD-DFT calculations correctly models the major solvent effects, such as electrostatic effects of the medium if no specific solute-solvent interaction is considered between solvent and solute (e.g., hydrogen bond interactions, dipole-dipole interactions, induced dipole-dipole interactions, etc.) [23]. Methanol (ε = 32.63) was chosen as this solvent was used for CD measurements. All calculations were performed using the Gaussian09 package [24]. Both GaussView [25] and VMD (Visual Molecular Dynamics) [26] were used for visualizing molecules. ECD spectra were graphically plotted using Gabedit software [27].

### Results and Discussion
Compound **1** was first analysed by NMR and HR-MS and led to the establishment of its plane structure. It was then crystallised from a MeOH/CHCl₃ mixture as red-orange crystals and subjected to X-ray diffraction analysis (Figure 3). As a result, its relative configuration was determined as rel-1*R*,2*S*,3*R*. Indeed, a diffractometer using short-wavelength radiation (Mo-Kα) to study a molecule containing only carbon, oxygen, and hydrogen atoms may not give dependable information on the absolute configuration.

The absolute configuration of compound **1** was determined by comparing its actual electronic circular dichroism (ECD) spectrum with one calculated by TD-DFT.
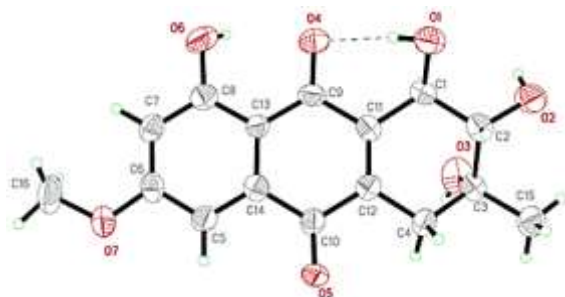
**Figure 3**. ORTEP of compound **1**

A conformational analysis was carried out for this latter purpose, and stable conformers for 4-dehydroxyaltersolanol A (**1**) were optimised using DFT. It led to four possible conformers and their Boltzmann distribution was determined considering their relative free energies (Figure 5). All conformers were subsequently geometry and energy-optimized by applying DFT using the hybrid B3LYP functional coupled with the 6–311+G(d,p) basis set that includes polarization and diffuse functions. Based on the optimized geometries of all four possible conformers for this secondary metabolite (**1**), TD-DFT formalism was performed to calculate the ECD spectra. We surveyed a range of functionals and basis sets, namely wB97XD, CAM-B3LYP, B3P86 and MO62X, and found that the M062X functional gave the best predictions to allow

comparison with experimentally obtained spectra (Figure 4). We used two broad classes of DFT functionals, as listed in Figure 4, those where a default correction for dispersion terms is included in the functional (M062X, ωB97XD) and a second class where such a correction is not included (B3P86, CAM-B3LYP), to evaluate the effect of dispersion on the ECD results. Moreover, we significantly increased the number of states computed for the time-dependent density-functional theory (TDDFT) from 30 previously to 250 (Figure 4). It is known that the 200−250 nm region can be poorly converged in terms of band shape if insufficient states are considered [28].

The ECD spectrum for each of the investigated conformers was built individually (Figure 5) and then merged by considering the contribution of each conformer in proportion to its Boltzmann distribution (Figure 6). The simulated spectrum of compound (**1**) using the 6-311++G(d,p) basis set and the M062X functional gave reasonably good agreement with the experimental spectrum, correctly predicting the positive and negative features, albeit with relative intensities that are not very well predicted (Figures 4 and 6). Both experimental and calculated curves were overlaid in Figure 6 and led to the unambiguous conclusion that **1** had the 1*S*,2*R*,3*S* configuration as correctly assumed by Uzor *et al*. [1].
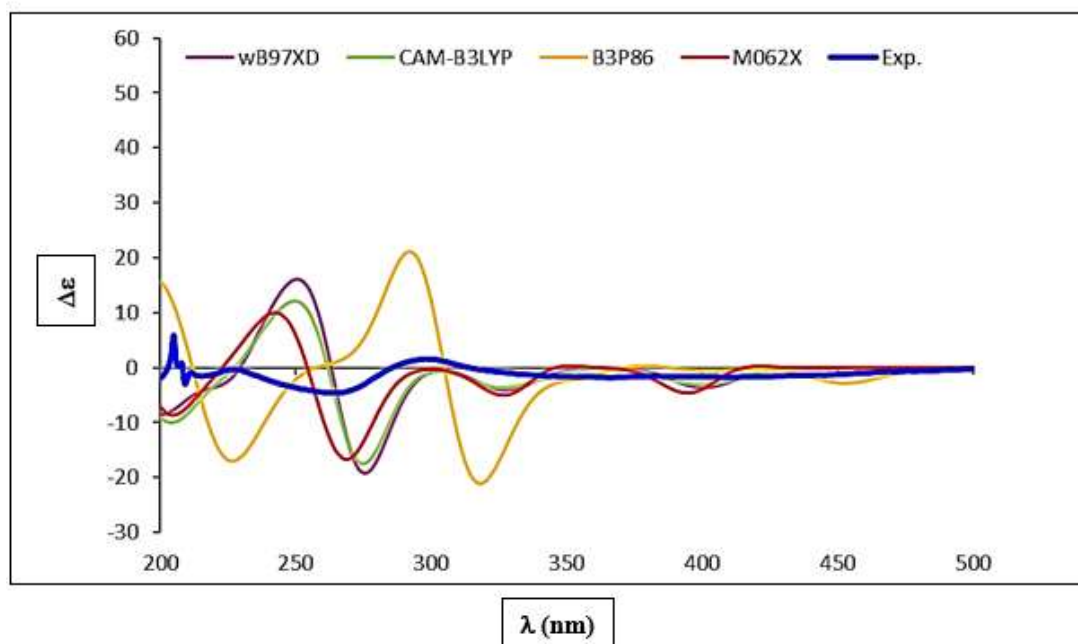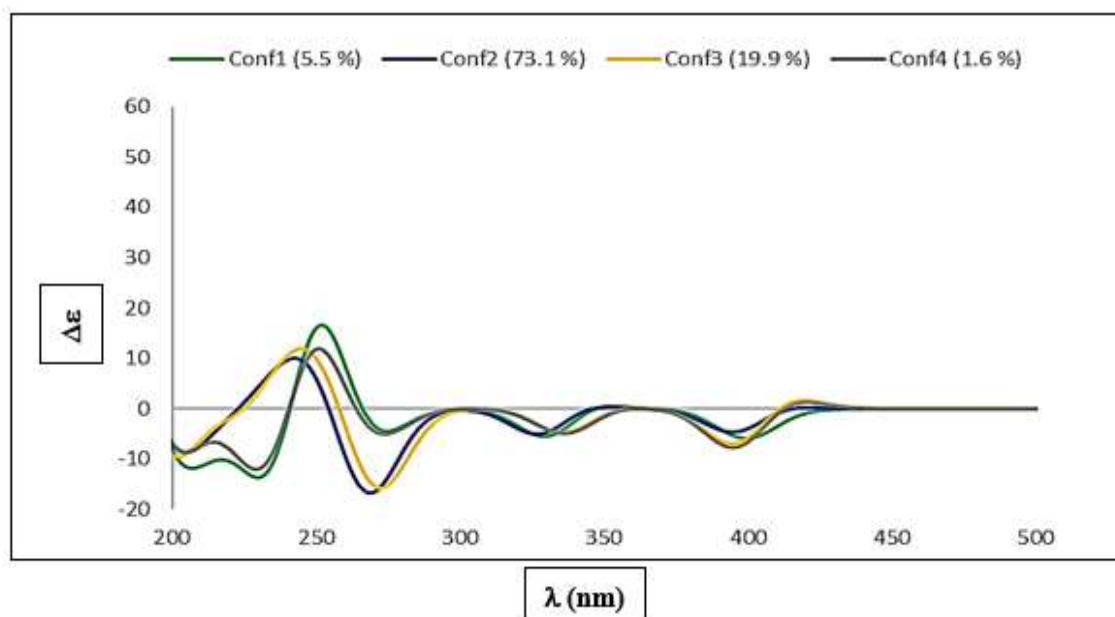


**Figure 4.** Calculated spectra of **1** in polarizable continuum model, using a range of functionals and the 6-311+ +G(d,p) basis set; the experimental curve is overlaid for comparison (blue curve).

**Figure 5.** Superposition of individual calculated (M062X/6-311++G(d,p)) electronic circular dichroism for all four optimized conformations

These results reveal that no uniform baseline shift can be applied that would bring the entire spectral range into exact agreement with the experimental trace for any of these functionals, and we therefore decided against trying to apply any such corrections as an aid to our interpretations. Although the agreement with the experiment for all these functionals might be good enough as evidence to assign the absolute configuration of the molecule, the changes between the different spectra are significant. Moreover, we wished to explore whether more subtle features of this structure such as aggregation, might be revealed by the ECD technique. In fact, the relatively poor agreement between the experimental and simulated data using the M062X functional in the 200-250 nm region may be justified by a possible hydrogen-bonded (HB) molecular dimer formation. After careful consideration of the 3D structure of **1**, we hypothesised that the possible formation of HB dimers D1 and D2 may be feasible (Figure 7).

The hydrogen-bonding network shown in Figure 7 has the potential to provide suitably strong interactions to ensure that the proposed molecular dimers are retained in solution. However, we do recognize that the range of concentrations and temperatures where ECD is usually recorded normally mitigate against dimer formation. Nevertheless, we believe that the difference between the monomer and dimer free energy would not be so large as to definitively exclude the possibility of a significant concentration of these dimers in solution. Since the formation of a molecular dimer would be expected to be concentration-and temperature-dependent, high concentrations would favor dimer formation, and temperature changes would be expected to perturb monomer/dimer equilibrium. A re-analysis of the mother liquor that afforded the crystals of 1 after a few weeks at lab temperature (24 °C) showed that **1** had all been converted into macrosporin (**4**).

We were drawn to suggest a mechanism for this conversion using quantum calculations. A double dehydration had taken place, thus leading to a more stable anthraquinone. The mechanism is initiated by the protonation of one of the three alcoholic groups, followed by the loss of a water molecule. A second similar dehydration would then follow. To determine the sequence of this double dehydration, the relative stabilities of protonated species on the 1-OH, 2-OH and 3-OH of **1** were calculated and compared using DFT. It appeared that protonation on 2-OH and 3-OH would lead to species that would have energies higher than the 1-OH protonated species (**8**, Figure 8) by 13.99 and 14.06 kcal/mol, respectively.
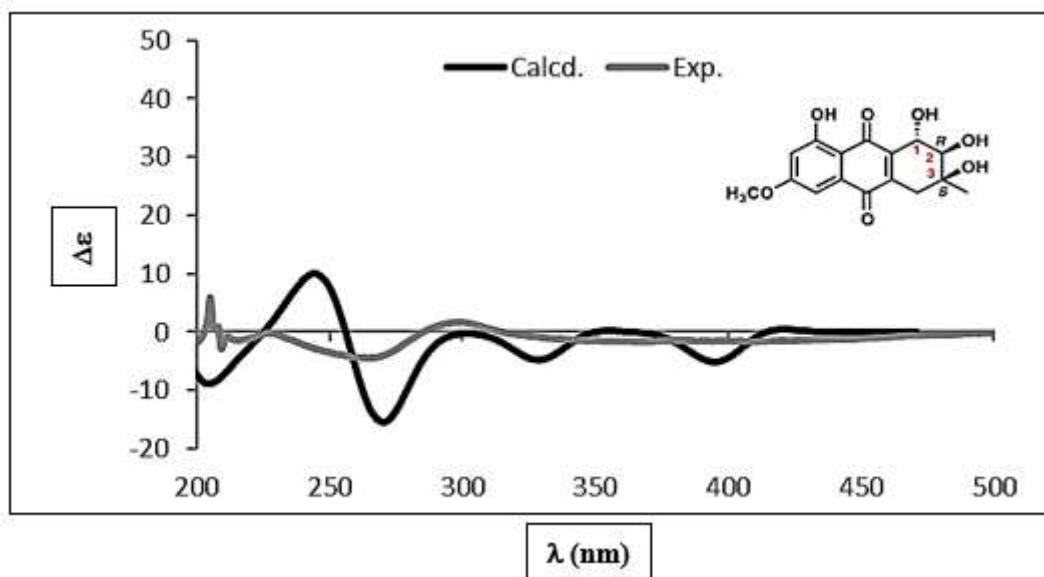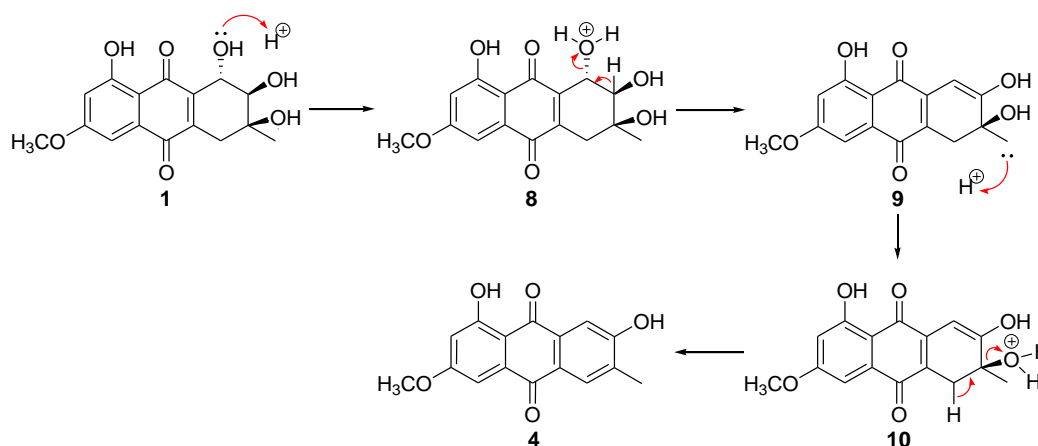
**Figure 6.** Experimental and calculated (M062X/6-311++G(d,p)) electronic circular dichroism pectra of compound **1**



(D1)

(D2)
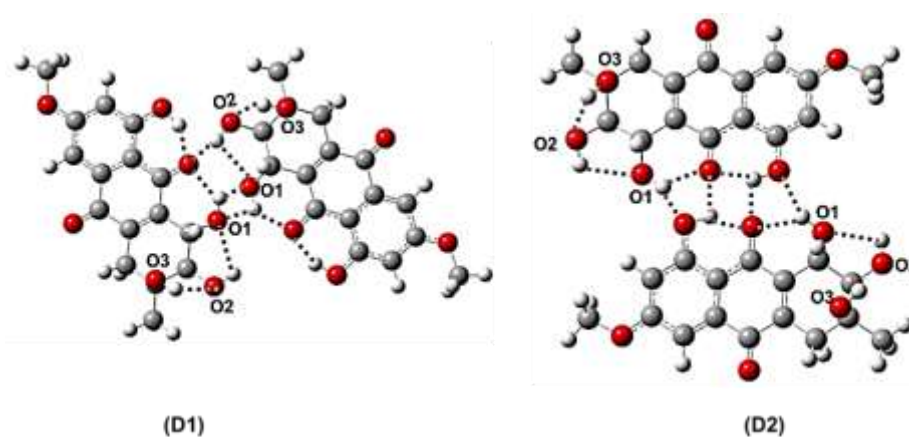
**Figure 7.** Hypothetic geometry of proposed HB dimers using conformer (3), namely D1 (a) and D2 (b); selected heteroatoms have been numbered to facilitate inspection of these structures



**Figure 8.** Proposed mechanism for the dehydration of 4-dehydroxyaltersolanol A (**1**) into macrosporin (**4**)

Therefore, it can be confidently proposed that the dehydration of **1** starts with its protonation on the 1-OH (species **7**), followed by the elimination of a water molecule leading to **8**. A second dehydration initiated by the protonation of the 3-OH (species **9**) is even further facilitated by the aromatization of the ring A. As a result of the above, it is uncertain whether macrosporin is a genuine natural product or just an artefact generated during the fermentation and/or isolation procedures.

### 4-Dehydroxyaltersolanol A (1)

red-orange crystals; mp 216 °C; $[\alpha]_D^{25}$ +27.3° (c 0.006, MeOH); UV (MeCN) $\lambda_{max}$ nm (log ε) 217 (3.89), 266 (3.52), 428 (3.02); $^1$H NMR (600 MHz, MeOD): 1.39 (s, H11), 2.63 (dd, 19.2 and 1.8 Hz, H4a), 2.81 (bd, 19.2 Hz, H4b), 3.65 (d, 5.4Hz, H2), 3.94 (s, 6-OMe), 4.86 (d, 5.4 Hz, H1), 6.75 (d, 2.4Hz, H7), 7.15 (d, 2.4 Hz, H5); $^{13}$C NMR (150 MHz, MeOD): 24.3 (C11), 35.2 (C4), 55.2 (6-OCH3), 69.0 (C1), 70.2 (C3), 76.9 (C2), 105.5 (C7), 107.0 (C5), 109.4 (C9a), 133.6 (C10a), 141.9 (C1a), 142.9 (C4a), 164.1 (C8), 166.1 (C6), 183.9 (C10), 188.4 (C9); ESI-TOF-MS m/z 319.0835 [M-H]$^-$ (calcd for $C_{16}H_{15}O_7$, 319.0818, ΔM = 0.0017 Da); ECD: (c 1.88x 10$^{-4}$ M, MeOH) λ(ε) nm 530(0), 407(-1.7), 315(0), 298(1.6), 285(0), 265( 4.5), 227(-0.2), 215(-1.5).

### Pestalopyrone (2)

Dark red, amorphous solid; mp 124 °C; $[\alpha]_D^{20}$ -15.0° (c 0.012, MeOH); UV (MeCN) $\lambda_{max}$ nm: 223, 309; HR-ESI-MS m/z 181.0850 [M+H]$^+$ (calcd for $C_{10}H_{13}O_3$, 181.0865, ΔM/M = 8.3 ppm); $^1$H NMR (600 MHz, MeOD, δ, ppm) δ 1.91 (3H, d, H-9), 1.89 (3H, s, H-10), 3.89 (3H, s, OCH$_3$), 5.60 (1H, d, J=1 Hz, H-5), 6.16 (1H, d, J=1 Hz, H-3), 6.66 (1H, q, J=7 Hz, H 8); $^{13}$C NMR (600 MHz, MeOD, δ, ppm) δ 172.7 (C-4), 165.6 (C-2), 161.3 (C-6), 129.6 (C-8), 126.9 (C-7), 97.4 (C-3), 87.2 (C-5), 55.6 (OCH$_3$-1), 12.9 (C-10), 10.7 (C-9).

### Hydroxypestalopyrone (3)

Dark brown, amorphous solid; mp 166 °C; $[\alpha]_D^{20}$ -15° (c 0.070, MeOH); HR ESI-MS m/z 197.0798 [M+H]$^+$ (calcd. 197.0814, ΔM/M = -8.1 ppm); $^1$H NMR (600 MHz, MeOD, δ, ppm) 1.92 (3H, d, J=1.5 Hz, H-9), 3.90 (3H, s, OCH3), 4.35 (1H, d, J=5.5 Hz, H-3 or H-5), 5.64 (1H, d, J=2.0 Hz. H-5 or H-3), 6.25 (1H, d, J=1.5 Hz, H-8), 6.63, t, J=4.5 Hz ; 13C NMR (600 MHz, MeOD,

δ, ppm) δ 172.4 (C-4), 165.2 (C-2), 160.5 (C-6), 133.6 (C-8), 126.7 (C-7), 98.6 (C-3), 87.8 (C-5), 58.2 (C-9), 55.6 (OCH$_3$-1), 11.1 (C-10).

### Macrosporin (4)

Yellow, amorphous powder; mp 177 °C;UV (MeCN) $\lambda_{max}$ nm: 225, 285, 380; HR-ESI-MS m/z 283.0613 [M-H]- (calcd for C16H12O5, 283.0606, ΔM/M = 2.5 ppm); 1H NMR (600 MHz, Acetone-d6, δ, ppm) δ 7.99 (1H, s, H 5), 7.67 (1H, s, H-8), 7.26 (1H, d, J=2.5 Hz, H-4), 6.73 (1H, d, J=2.5 Hz, H-2), 4.00 (3H, s, OCH3-3), 2.37 (3H, s, CH3-6); 13C NMR (600 MHz, Acetone-d6, δ, ppm) δ 187.3 (C 9), 180.5 (C-10), 166.4 (C-3), 165.8 (C-1), 162.1 (C-7), 136.2 (C-4a), 133.7 (C-8a), 132.5 (C-6), 130.2 (C-5), 123.5 (C-10a), 111.5 (C-8), 110.3 (C-9a), 107.0 (C-4), 105.2 (C-2), 55.7 (OCH$_3$-3), 15.7 (CH$_3$-6).

### Altersolanol B (6)

Red needles like crystal, mp 228 °C, $[\alpha]_D^{20}$ -12° (c 0.171, MeOH); UV (MeCN) $\lambda_{max}$ nm: 217, 265, 285, 421; HR-ESI-MS m/z 305.1019 [M+H]$^+$ (calcd for $C_{16}H_{17}O_6$, 305.1025, ΔM/M = 2.0 ppm); $^1$H-NMR (600 MHz, CDCL$_3$, δ, ppm) 7.36( d, J=2.5 Hz), 6.71( d, J=2.5 Hz), 3.94, s, 3.50 (dd, J=11.8, 4.5 Hz), 2.39 ( ddd, 12.8, 4.5, 3.7), 2.27 (dd, 14.2, 3.5), 1.84 (dt, 12.8, 11.8), 1.60 ( dd, 14.2, 11.6), 1.31 (s).

### Crystallographic data for 1

$C_{16}H_{16}O_7$, M = 320.29, orthorhombic, a = 10.365(10) Å, b = 24.259(2) Å, c = 5.619(6) Å, α = 90°, β = 90°, γ = 90°, V = 1412.9(2) Å3, T = 302(2) K, space group P21212, Z = 4, μ (Mo Kα) = 0.119 mm$^{-1}$, 20715 reflections measured, 2628 independent reflections (Rint = 0.1682). The final R1 value was 0.0952 [I > 2σ(I)]. The final wR(F2) value was 0.1711 [I > 2σ(I)]. The final R1 value was 0.1240 (all data). The final wR(F2) value was 0.1869 (all data). The goodness of fit on F2 was 1.181.

A standard technique was used for the isolation of endophytic fungi from Malaysian plants. The analysis of the secondary metabolism of the isolates obtained during this project was purposely limited to the major components. The very minor compounds from the four selected extracts possibly deserve attention. Future research undertaken shall go beyond this limitation to observe possibilities of new compounds.

## Conclusion

The combination of X-ray crystallography, ECD and TD-DFT allowed unambiguously assigning the absolute stereochemistry of 4 dehydroxyaltersolanol A as 1*S*,2*R*,3*S* as correctly assumed by Proksh and collaborators from biogenetic considerations. While conventional wisdom calls for a given organism to biosynthesise only compounds with the same stereochemistry, there are quite several examples of biosynthetic enantiodivergence where the organism produces metabolic congeners as enantiomers, diastereoisomers or moieties of opposite configuration.

## Author contributions

Fatimah Bebe Mohamed Hussain actively isolated all the compounds and performed the bench work; Imene Bayach, Fatimah Salim Syed Adnan Ali Shah and Kamran Ashraf assisted for NMR, ECD and TD-DFT quantum calculations; Humera Naz helped for X-ray diffraction; Sadia Sultan and Jean-Frédéric Faizal Weber proposed the study design, provided conceptual and technical guidance, and assisted in the preparation and writing of the manuscript; Gurmeet Kaur helped in revising and improved the write-up. All authors read and agreed to the final version of the manuscript.

## Declaration of interest

The authors declare that there is no conflict of interest. The authors alone are responsible for the accuracy and integrity of the paper content.

## References

[1] Uzor PF, Ebrahim W, Osadebe PO, Nwodo JN, Okoye FB, Müller WEG, Lin W, Liu Z, Proksch P. Metabolites from *Combretum dolichopetalum* and its associated endophytic fungus *Nigrospora oryzae* -Evidence for a metabolic partnership. *Fitoterapia*. 2015; 105: 147–150.

[2] Strobel GA. Rainforest endophytes and bioactive products. *Crit Rev Biotechnol*. 2002; 22(4): 315–333.

[3] Sultan S, Sun L, Blunt JW, Cole ALJ, Munro MHG, Ramasamy K, Weber JFF. Evolving trends in the dereplication of natural product extracts. 3: Further lasiodiplodins from *Lasiodiplodia theobromae*, an endophyte from *Mapania kurzii. Tetrahedron Lett*. 2014; 55(2): 453–455.

[4] Ou SH. Rice diseases. Commonwealth Mycological Institute. Kew: Surrey, 1985.

[5] Neergaard P. Seed pathology. London: The Macmillan Press Ltd, 1977.

[6] Wu JB, Zhang CL, Mao PP, Qian YS, Wang HZ. First report of leaf spot caused by *Nigrospora oryzae* on *Dendrobium candidum* in China. *Plant Dis*. 2014; 98(7): 996–998.

[7] Zhang LX, Li SS, Tan GJ, Shen JT, He T. First report of *Nigrospora oryzae* causing leaf spot of cotton in China. *Plant Dis*. 2012; 96(9): 1379.

[8] Sharma P, Meena PD, Chauhan JS. First report of *Nigrospora oryzae* (Berk. & Broome) Petch causing stem blight on *Brassica juncea* in India. *J Phytopathol*. 2013; 161(6): 439–441.

[9] Saunders M, Kohn LM. Host-synthesized secondary compounds influence the *in vitro* interactions between fungal endophytes of maize. *Appl Environ Microbiol*. 2008; 74(1): 136–142.

[10] Li D, Chen Y, Pan Q, Tao M, Zhang W. A new eudesmane sesquiterpene from *Nigrospora oryzae*, an endophytic fungus of *Aquilaria sinensis. Rec Nat Prod*. 2014; 8(4): 330–333.

[11] Szewczuk V, Kita W, Jarosz B, Truszkowska W, Siewiński AJ. Growth inhibition of some phytopathogenic fungi by organic extracts from *Nigrospora oryzae* (Berkeley and Broome). *Basic Microbiol*. 1991; 31(1): 69–73.

[12] Rathod DP, Dar MA, Gade AK, Rai MK. Griseofulvin producing endophytic *Nigrospora Oryzae* from Indian *Emblica officinalis* Gaertn: a new report. *Austin J Biotechnol Bioeng*. 2014; 1(6): 1–5.

[13] Tanaka M, Fukushima T, Tsujino Y, Fujimori T. Nigrosporins A and B, new phytotoxic and antibacterial metabolites produced by a fungus *Nigrospora oryzae. Biosci Biotechnol Biochem*. 1997; 61(11): 1848–1852.

[14] Venkatasubbaiah P, Van Dyke CG, Chilton WS. Phytotoxins produced by *Pestalotiopsis*

*oenotherae*, a pathogen of evening primrose. *Phytochemistry*. 1991; 30(5): 1471–1474.

[15] Lee JC, Yang X, Schwartz M, Strobel G, Clardy J. The relationship between an endangered North American tree and an endophytic fungus. *Chem Biol*. 1995; 2(11): 721–727.

[16] Suemitsu R, Nakajima M, Hiura M. Studies on the metabolic products of *Macrosporium porri* Elliott Part III. Structure of macrosporin (group II). *Bull Agric Chem Soc Jpn*. 1959; 23(6): 547–551.

[17] Nakajima S. Studies on the metabolites of phytotoxic fungi. I. Isolation of macrosporin and 6-methylxanthopurpurin 3-methyl ether from *Alternaria bataticola* Ikata ex Yamamoto. *Chem Pharm Bull*. 1973; 21(9): 2083–2085.

[18] Suemitsu R, Ohnishi K, Yanagawase S, Yamamoto K, Yamada Y. Biosynthesis of macrosporin by *Alternaria porri*. *Phytochemistry*. 1989; 28(6): 1621–1622.

[19] Stoessl A. Some metabolites of *Alternaria solani*. *Can J Chem*. 1969; 47: 767–776.

[20] Noda T, Take T, Watanabe T, Abe J. The structure of bostrycin. *Tetrahedron*. 1970; 26(6): 1339–1346.

[21] Sheldrick GM. A short history of SHELX. *Acta Crystallogr A*. 2008; 64(Pt 1): 112–122.

[22] Sheldrick GM. SHELXL2013, Göttingen: University of Göttingen, 2013.

[23] Jacquemin D, Wathelet V, Perpete EA, Adamo C. Extensive TD-DFT benchmark: singlet-excited states of organic molecules. *J Chem Theory Comput*. 2009; 5(9): 2420–2435.

[24] Frisch MJ, Trucks GW, Schlegel HB, Scuseria GE, Robb MA, Cheeseman JR, Scalmani G, Barone V, Mennucci B, Petersson GA, Nakatsuji H, Caricato M, Li X, Hratchian HP, Izmaylov AF, Bloino J, Zheng G, Sonnenberg JL, Hada M, Ehara M, Toyota K, Fukuda R, Hasegawa J, Ishida M, Nakajima T, Honda Y, Kitao O, Nakai H, Vreven T, Montgomer JA Jr, Peralta JE, Ogliaro F, Bearpark M, Heyd JJ, Brothers E, Kudin KN, Staroverov VN, Kobayashi R, Normand J, Raghavachari K, Rendell A, Burant JC, Iyengar SS, Tomasi J, Cossi M, Rega N, Millam JM, Klene M, Knox JE, Cross JB, Bakken V, Adamo C, Jaramillo J, Gomperts R, Stratmann RE, Yazyev O, Austin AJ, Cammi R, Pomelli C, Ochterski JW, Martin RL, Morokuma K, Zakrzewski VG, Voth GA, Salvador P, Dannenberg JJ, Dapprich S, Daniels AD, Farkas Ö, Foresman JB, Ortiz JV, Cioslowski J, Fox DJ. Gaussian 09, Revision A.02. Wallingford: Gaussian Inc, 2009.

[25] Dennington R, Keith T, Millam J. GaussView, Version 5.0.8.: Semichem Inc., Shawnee Mission KS, 2009.

[26] Humphrey W, Dalke A, Schulten K. VMD: visual molecular dynamics. *J Mol Graph*. 1996; 14(1): 33–38.

[27] Allouche AR. Gabedit - A graphical user interface for computational chemistry softwares. *J Comput Chem*. 2011; 32(1): 174–182.

[28] Di Bari L, Pescitelli G. Electronic circular dichroism. In: Computational spectroscopy-methods, experiments and applications. Grunenberg J, Ed. Weinheim: Wiley-VCH, 2010.

## Abbreviations

ECD: electronic circular dichroism; TD-DFT: time-dependent density-functional theory; DFT: density-functional theory; NMR: nuclear magnetic resonance; $CD_3OD$: deuterated methanol; $CDCl_3$: deuterated chloroform; TOF LC/MS: time-of-flight liquid chromatography/mass spectrometry; UV: ultra-violet; FRIM: Forest Research Institute of Malaysia; PCR: polymerase chain reaction; PDA: potato dextrose agar; MeOH: methanol; ACN: acetonitril; CCDC: Cambridge Crystallographic Data Centre; PCM: polarizable continuum model; VMD: visual molecular dynamics